

# Entanglement assisted spin-wave atom interferometer

Yu-Ao Chen,<sup>1,2</sup> Xiao-Hui Bao,<sup>1,2</sup> Zhen-Sheng Yuan,<sup>1,2</sup> Shuai Chen,<sup>1</sup> Bo Zhao,<sup>1</sup> and Jian-Wei Pan<sup>1,2</sup>

<sup>1</sup>*Physikalisches Institut, Ruprecht-Karls-Universität Heidelberg, Philosophenweg 12, 69120 Heidelberg, Germany*

<sup>2</sup>*Hefei National Laboratory for Physical Sciences at Microscale and Department of Modern Physics, University of Science and Technology of China, Hefei, Anhui 230026, China*

(Dated: November 12, 2018)

We report the observation of phase-super resolution in a motion-sensitive spin-wave (SW) atom interferometer utilizing a NOON-type entangled state. The SW interferometer is implemented by generating a superposition of two SWs and observing the interference between them, where the interference fringe is sensitive to the atomic collective motion. By heralded generation of a second order NOON state in the SW interferometer, we clearly observe the interference pattern with phase super-resolution. The demonstrated SW interferometer can in principle be scaled up to highly entangled quantum state, and thus is of fundamental importance to implement quantum-enhanced-measurement.

PACS numbers: 06.30.Gv, 03.75.Dg, 37.25.+k

The optical interferometer [1] and the atom interferometer [2] have become essential tools for measuring position, displacement or acceleration. In these devices, a classical light pulse or an ensemble of neutral atoms are coherently split and recombined in space domain or time domain by applying mechanical or optical gratings. The gravity or platform rotation will cause a motion-sensitive phase shift, which can be measured from the interference fringes.

As is well known, by exploiting suitable quantum entanglement, e.g. NOON state or GHZ state, the measurement precision can be improved [1, 3]. For optical interferometers, the principle of the quantum-enhanced-measurement has been demonstrated by exploiting photonic NOON state, where phase super-resolution [4, 5] and phase super-sensitivity [6] have been observed for  $N=4$ . However, generating atomic NOON state or GHZ state and exploiting them in atom interferometers are still challenging for current technology. Although entanglement up to eight atoms has been achieved in ion traps [7], this system can not be exploited in conventional motion-sensitive atom interferometers due to the fact that the atoms have to be ionized and confined in a small volume.

Here we propose and demonstrate a motion-sensitive entanglement-assisted SW atom interferometer. In our protocol, instead of using superposition of single atoms, we exploit superposition of the collective excited states, i.e. the SW, to implement the interferometer. The collective motion of the atoms will cause a phase shift, which can be measured by converting the SW into photons. The SW interferometer is experimentally demonstrated by using cold atomic ensembles, where the collective motion is introduced by a radiation pressure force. Further, we heralded generate a second order NOON state in the SW interferometer. The motion sensitivity is proved to be twice higher, which clearly shows the phase super-resolution. Our method can lead to phase super-sensitivity with the

improvement of coherence time of the SWs. Moreover, the SW interferometer can in principle be scaled up to highly entangled states, which might be useful in inertial sensing.

To illustrate the working scheme of SW interferometer, we consider a cold atomic cloud with the  $\Lambda$ -type level structure shown in the Fig. 1. All the atoms are initially optically pumped to  $|g\rangle$ . An off-resonant  $\sigma^-$  polarized write pulse coupling the transition  $|g\rangle \rightarrow |e\rangle$  with wave vector  $\mathbf{k}_w$  is applied to the atomic ensemble along the axial direction, inducing spontaneous Raman scattering. Two Stokes fields with  $\sigma^-$  polarization and wave vector  $\mathbf{k}_{sa}$  and  $\mathbf{k}_{sb}$  are collected at an angle of  $\theta_{a,b} = \pm\theta$  relative to the write beam. The atom-light field in each mode can be expressed as [8]

$$|\Psi\rangle_i \sim |0\rangle_i^s |0\rangle_i + \sqrt{\chi_i} |1\rangle_i^s |1\rangle_i + \chi_i |2\rangle_i^s |2\rangle_i + O(\chi_i^{3/2}), \quad (1)$$

where  $\chi_a = \chi_b \ll 1$  is the excitation probability of one collective spin excitation in mode  $i$  ( $i = a, b$ ),  $|j\rangle_i^s$  denotes the the Stokes field  $S_i$  with photon number  $j$ , while  $|j\rangle_i = S_i^{\dagger j} |0\rangle_i$  denotes the  $j$ -fold collective spin excitation in mode  $i$ , with  $|0\rangle_i = \bigotimes_l |g\rangle_l$  the vacuum,  $S_i^\dagger = \frac{1}{\sqrt{M_i}} \sum_l e^{i\Delta\mathbf{k}_i \cdot \mathbf{r}_l^i} |s\rangle_l \langle g|$  the creation operator of SW $_i$ , where  $\Delta\mathbf{k}_i = \mathbf{k}_w - \mathbf{k}_{si} \simeq \mathbf{k}_w \sin \theta_i$  is the wave vector of SW $_i$  and  $\mathbf{r}_l^i$  denotes the coordinate of the  $l$ -th atom in mode  $i$ .

The two Stokes fields are rotated to be horizontally ( $|H\rangle$ ) and vertically ( $|V\rangle$ ) polarized for mode  $a$  and  $b$  respectively, and are combined on a polarized beam splitter (PBS). The half-wave plate (HWP $_s$ ) is set to  $22.5^\circ$  to measure the Stokes photons under  $|\pm\rangle = \frac{1}{\sqrt{2}}(|H\rangle \pm |V\rangle)$  basis. Neglecting high order excitations, a click on detector D $_{s1}$  or D $_{s2}$  will project the atomic ensembles into the superposition state

$$|\Psi\rangle = \frac{1}{\sqrt{2}}(|1\rangle_a |0\rangle_b \pm |0\rangle_a |1\rangle_b). \quad (2)$$

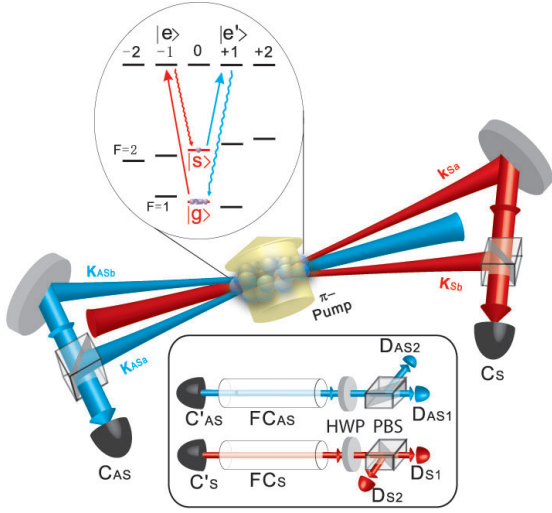


FIG. 1: Experimental setup of the SW interferometer. The inset at the top shows the relevant Zeeman levels for the  $|5S_{1/2}\rangle \rightarrow |5P_{1/2}, F'=2\rangle$  transition of  $^{87}\text{Rb}$  atoms. Before the experimental cycles we optically pump the atoms in  $|g\rangle$  by applying two pumping lights (See Appendix for detail.), one of which is shining in from the lateral side ( $\pi$ -Pump) to introduce radiation pressure force. A weak  $\sigma^-$  polarized write pulse is applied to generate two modes of SW and Stokes fields via spontaneous Raman transition  $|g\rangle \rightarrow |e\rangle \rightarrow |s\rangle$ . The Stokes fields are collected at the angle of  $\pm 0.6^\circ$  relative to the write beam, combined on a PBS and directed into a single mode fiber via a fiber coupler ( $C_S$ ). After a controllable delay, a strong  $\sigma^+$  polarized read beam induces the transition  $|s\rangle \rightarrow |e'\rangle \rightarrow |g\rangle$ , converting the two SWs into two anti-Stokes fields, which are overlapped in another PBS and then directed to a coupler ( $C_{AS}$ ). Passing through two filter cells (FC) respectively, the anti-Stokes photon from  $C'_{AS}$  and Stokes photon from  $C'_S$  are then sent to the polarization analyzers combined with half wave plate (HWP), polarized-beam splitter (PBS) and single photon detectors (D), as illustrated in the inset at bottom. Filter cells are properly pumped in order to absorb the remaining leakage from read or write beams while to be transparent for the signals.

Such a SW superposition state can be exploited to implement the Mach-Zehnder interferometer.

Assume the atoms undergo a collective motion, e.g. motion caused by gravitational acceleration, described as  $\mathbf{r}_i^t = \mathbf{r}_i^i + \mathbf{r}_c$ . Since  $|1\rangle_i = S_i^\dagger |0\rangle_i = \frac{1}{\sqrt{M_i}} \sum_l e^{i\Delta\mathbf{k}\cdot\mathbf{r}_l^i} |g\dots s_l\dots g\rangle$ , after the collective motion the SW will change to  $|1'\rangle_i = e^{i\phi_i} |1\rangle_i$  with  $\phi_i = \Delta\mathbf{k}_i \cdot \mathbf{r}_c$ , where  $\Delta\mathbf{k}_a = -\Delta\mathbf{k}_b \equiv \Delta\mathbf{k}$ . Thereby, we obtain

$$\begin{aligned} |\Psi'\rangle &= \frac{1}{\sqrt{2}} (e^{i\Delta\phi} |1\rangle_a |0\rangle_b \pm e^{-i\Delta\phi} |0\rangle_a |1\rangle_b) \\ &\sim \frac{1}{\sqrt{2}} (|1\rangle_a |0\rangle_b \pm e^{-i2\Delta\phi} |0\rangle_a |1\rangle_b), \end{aligned} \quad (3)$$

with  $\Delta\phi = \Delta\mathbf{k} \cdot \mathbf{r}_c$ . It can be readily seen that the collective motion of the atoms is mapped to a relative phase

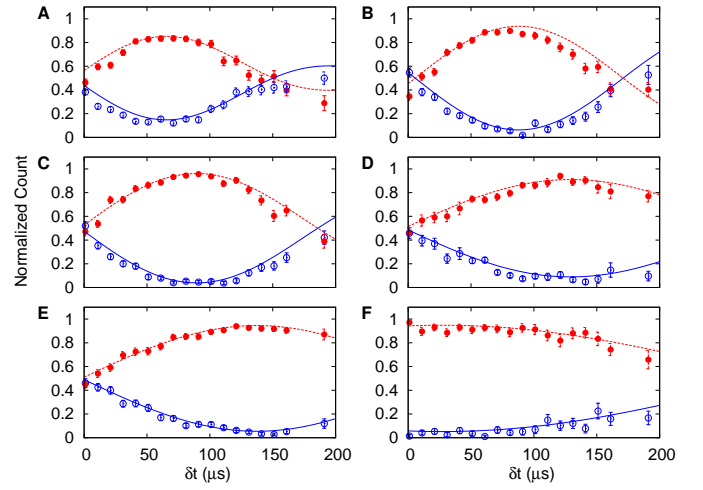


FIG. 2: The fidelity of anti-Stokes field on  $|+\rangle$  as a function of  $\delta t$ . Solid circles (open circles) represents the measured fidelity of anti-Stokes field on  $|+\rangle$  ( $|-\rangle$ ). The power of the  $\pi$ -Pump is: (A) 6 mW, (B) 4.5 mW, (C) 3 mW, (D) 1.5 mW, (E) 0.75 mW, (F) 0 mW. The experimental data are jointly fitted by using  $f_{|+\rangle}(\delta t) = (0.5 + a \sin^2(\pi \frac{t}{T} + \phi_0) e^{-\delta t^2/\tau^2}) / (1 + a e^{-\delta t^2/\tau^2})$  and  $f_{|-\rangle}(\delta t) = (0.5 + a \cos^2(\pi \frac{t}{T} + \phi_0) e^{-\delta t^2/\tau^2}) / (1 + a e^{-\delta t^2/\tau^2})$  (See Appendix for detail.). The evolution period  $T = \frac{\pi}{\Delta\mathbf{k} \cdot \mathbf{v}_c}$  is measured to be (A)  $317 \pm 18 \mu\text{s}$ , (B)  $330 \pm 15 \mu\text{s}$ , (C)  $378 \pm 14 \mu\text{s}$ , (D)  $555 \pm 47 \mu\text{s}$ , (E)  $591 \pm 30 \mu\text{s}$ , (F)  $1177 \pm 152 \mu\text{s}$ . Error bars represent statistical errors, which are  $\pm 1$  s.d.

in the superposition state. This phase and thus the collective motion can be measured by converting the SW back into photons and observing the interference pattern of the SW interferometer. In this way, if  $\Delta\mathbf{k}$  is set in the direction of the gravity, one can measure the gravitational acceleration. Moreover, any quantity regarding to center of mass displacements can be measured. The measurement precision is corresponding to the sensitivity of the interferometer determined by length of the wave vector  $\Delta\mathbf{k}$ , which is controllable in practice.

Such a single-excitation SW interferometer can be looked upon as the first order of a NOON state [9]. Higher order NOON state can be deterministically generated by using the linear optical methods (See Appendix for detail.), described as

$$|\text{NOON}\rangle = \frac{1}{\sqrt{2}} (|N\rangle_a |0\rangle_b + |0\rangle_a |N\rangle_b),$$

where  $|N\rangle_i = S_i^{\dagger N} |0\rangle_i$  denotes the  $N$ -fold excitation in mode  $i$  ( $i = a, b$ ). Thus the collective motion of the atoms will induce a phase as

$$|\text{NOON}'\rangle \sim \frac{1}{\sqrt{2}} (|N\rangle_a |0\rangle_b + e^{-i2N\Delta\phi} |0\rangle_a |N\rangle_b).$$

Note that, although the method for preparing NOON state is in principle extendable [4] to arbitrary  $N$ , the

efficiency of generating the desired NOON state drops off exponentially [9] with  $N$ . In order to be more efficient in employing entanglement, one can exploit multiple atomic ensembles to prepare  $N$ -quanta Greenberger-Horne-Zeilinger (GHZ) state [10]

$$|\text{GHZ}\rangle = \frac{1}{\sqrt{2}}(|1\rangle_{a_1}|0\rangle_{b_1}\dots|1\rangle_{a_N}|0\rangle_{b_N} + |0\rangle_{a_1}|1\rangle_{b_1}\dots|0\rangle_{a_N}|1\rangle_{b_N}),$$

which can be deterministically generated in a scalable way [11, 12], thanks to the built in quantum memory. The collective motion of the atoms will induce a phase as

$$|\text{GHZ}'\rangle \sim \frac{1}{\sqrt{2}}(|1\rangle_{a_1}|0\rangle_{b_1}\dots|1\rangle_{a_N}|0\rangle_{b_N} + e^{-i2N\Delta\phi}|0\rangle_{a_1}|1\rangle_{b_1}\dots|0\rangle_{a_N}|1\rangle_{b_N}).$$

Therefore, the SW interferometer would be  $N$  times more sensitive to the collective motion with the help of these highly entangled states and thus can be exploited to demonstrate the phase super-resolution and phase super-sensitivity.

Demonstration of the SW interferometers critically depends on the coherence time of the SW excitation. In the experiment, we implement the SW interferometer with  $^{87}\text{Rb}$  atoms trapped in a MOT at a temperature of about 100  $\mu\text{K}$ . By exploiting the clock transitions of,  $|g\rangle = |5S_{1/2}, F=1, m_F=0\rangle$  and  $|s\rangle = |5S_{1/2}, F=2, m_F=0\rangle$  as the two ground states to avoid the deleterious effects induced by magnetic field, e.g. Larmor precession or inhomogeneous broadening, we achieve the coherence time of the SW of about 200  $\mu\text{s}$ , which is limited by the dephasing of the SW induced by atomic random motion [13]. With such a coherence time, it is now possible to experimentally study the motion sensitivity of the SW interferometer.

To show the motion sensitivity, we introduce a collective motion during the pumping stage, where the atoms absorb photons from the  $\pi$ -Pump light and the  $2 \rightarrow 2$  pump, and then decay spontaneously. Since the  $2 \rightarrow 2$  pump is shined with the cooler light from six directions, and spontaneous emission is in arbitrary directions, on average they give no contribution to the collective motion. While the  $\pi$ -Pump light from the lateral side acts as a pushing laser, which causes a radiation pressure force and accelerates the atoms [14] until they are pumped to  $|g\rangle$ . We denote the velocity acquired in this process by  $\mathbf{v}_p = v_p \hat{\mathbf{e}}_p$ . Besides, the unbalance of other lasers, i.e. cooler, repumper, and etc., will also induce an initial velocity  $\mathbf{v}_0$  when the atoms are released. Note that, both of the modes  $a$  and  $b$  are accelerated by the pushing laser. Therefore when the the superposition state  $|\Psi\rangle$  (Eq. 2) is generated, it will evolve to  $|\Psi'\rangle$  (Eq. 3) after a free evolution time of  $\delta t$ , where  $\Delta\phi = \Delta\phi(\delta t) = \Delta\mathbf{k} \cdot \mathbf{v}_c \delta t$  with  $\mathbf{v}_c = \mathbf{v}_p + \mathbf{v}_0$  and in which the atomic random motion is neglected.

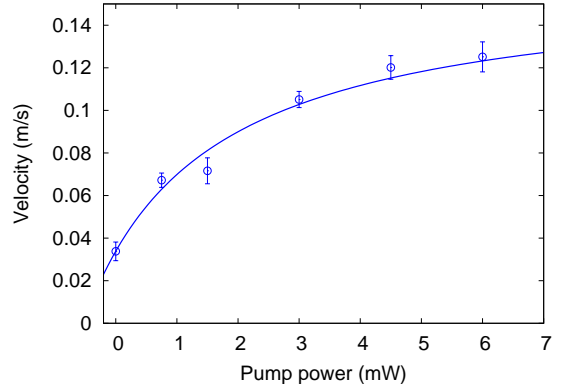


FIG. 3: The atomic velocity as a function of the  $\pi$ -Pump power. The initial velocity induced by the unbalance of other lasers is about 0.03 m/s. The velocity acquired in the pumping stage increases with the pumping power until reaching a plateau of about 0.12 m/s. Error bars represent statistical errors, which are  $\pm 1$  s.d.

To measure  $\Delta\phi(\delta t)$ , a strong  $\sigma^+$  polarized read light, coupling the transition  $|e'\rangle \rightarrow |g\rangle$ , counter-propagating with the write light, converts the collective excitations into  $\sigma^+$  polarized anti-Stokes fields. The anti-Stokes fields from two atomic ensembles are rotated to be perpendicular to each other and combined on a PBS (Fig. 1), which can be described by  $|\Psi\rangle_{\text{AS}} \sim \frac{1}{\sqrt{2}}(|H\rangle_{\text{AS}} \pm e^{-i(2\Delta\phi(\delta t))} e^{i(\phi_1 + \phi_2)} |V\rangle_{\text{AS}})$ , where  $\phi_1$  ( $\phi_2$ ) represents the propagating phase difference between two Stokes (anti-Stokes) fields before overlapping. Note that in the experiment, the total phase  $\phi_1 + \phi_2$  is actively stabilized and set to a fixed value [15]. The interference pattern is observed by setting the HWP<sub>AS</sub> at 22.5° to detect the anti-Stokes fields under  $+/ -$  basis. We change the power of the  $\pi$ -pump and measure the fidelity of anti-Stokes field on  $|+\rangle$  as a function of  $\delta t$ , on condition of a click of Stokes field on state  $|+\rangle$  (solid circles) and  $|-\rangle$  (open circles). The experiment results are shown in Fig. 2, where the data are fitted by taking into account the retrieve efficiency and the background noise (See Appendix for detail.). The collective motion can be obtained from the period of the interference pattern  $T = \frac{\pi}{\Delta\mathbf{k} \cdot \mathbf{v}_c}$ , which varies from 300  $\mu\text{s}$  to 1200  $\mu\text{s}$ .

The velocity that the atoms acquired as a function of the  $\pi$ -Pump power is shown in Fig. 3. One can see that the average velocity will first increase with the  $\pi$ -Pump power, and reach a plateau when the  $\pi$ -Pump is sufficient strong. This might be related with the pumping efficiency in the pumping stage, since when all the atoms are pumped to the  $|g\rangle$ , the atoms will not absorb photons from  $\pi$ -Pump any more. Note that, the population in other Zeeman sub-levels arising from insufficient pump will not affect the interference pattern since the decoherence time in other states is very short (about mi-

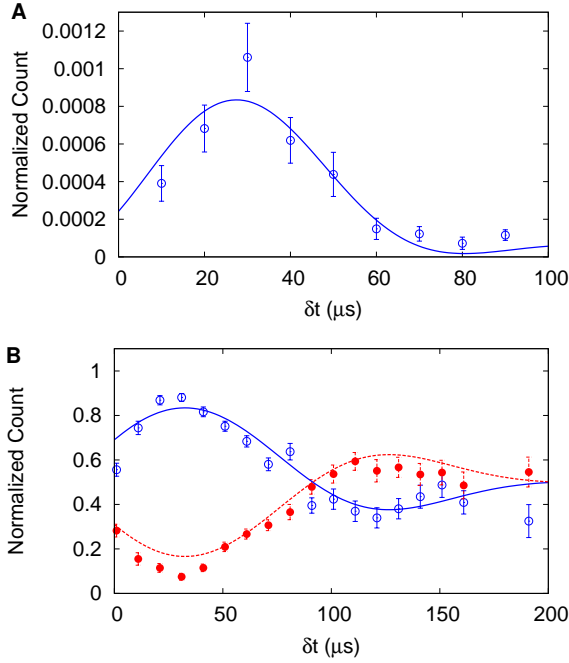


FIG. 4: Comparison of the performance of the first and second order NOON state. **(A)**, The normalized coincidence count for the second order NOON state as a function of  $\delta t$ . The experimental data are fitted by using  $c(\delta t) = b \sin^2(\pi \frac{\delta t}{T'} + \phi'_0) e^{-2\delta t^2/\tau'^2} + d e^{-\delta t^2/\tau'^2}$  (See Appendix for detail.). The fitting evolution period is  $T' = (94 \pm 12) \mu s$ . **(B)**, The interference pattern for  $N = 1$  under the same condition. The lines are the fitted with the same method as in Fig. 2. The fitting evolution period is  $T = (220 \pm 17) \mu s$ , which is about twice high as  $T'$ . Error bars represent statistical errors, which are  $\pm 1$  s.d.

croseconds) due to inhomogeneous broadening.

To experimentally show the advantage of quantum entanglement, we generate the second order NOON state, which can be described as  $|\Psi\rangle_{NOON} = \frac{1}{\sqrt{2}}(|2\rangle_a|0\rangle_b - |0\rangle_a|2\rangle_b)$ . This is achieved by registering the coincidence count between single photon detectors  $D_{S1}$  and  $D_{S2}$  (See Appendix for detail.). Note that, such a state is deterministically generated with the help of a feedback circuit [16]. After a free evolution time of  $\delta t$ , we have  $|\Psi\rangle_{NOON'} \sim \frac{1}{\sqrt{2}}(|2\rangle_a|0\rangle_b - e^{-i(4\Delta\phi(\delta t))}|0\rangle_a|2\rangle_b)$ . By converting the second order state to anti-Stokes fields and measuring the coincidence count between detectors  $D_{AS1}$  and  $D_{AS2}$ , we obtain the phase  $\Delta\phi(\delta t)$ . The normalized coincidence count is shown in Fig. 4A. For comparison, we give the interference fringe for the first order NOON state under the same condition as shown in Fig. 4B, which is taken directly after the measurement of the second order interference pattern. It can be seen that the evolution period of second order NOON state (Fig. 4A,  $T' = (94 \pm 12) \mu s$ ) is about 1/2 of the first order (Fig. 4B,  $T = (220 \pm 17) \mu s$ ), which clearly shows the phase

super-resolution. Note that, these data are taken under  $\pi$ -pump power of 6 mW. There's a slightly change of the initial velocity of the atomic ensemble compared to the original condition, which makes the first order evolving period slightly different to the one given in Fig. 2A.

With emphasis, we note that NOON state is not only more sensitive to the collective motion, but also more sensitive to decoherence [1, 17]. Therefore, to achieve phase super-sensitivity, the coherence time of our NOON state has to be much larger than its free evolution time [18, 19]. However, in our experiment, since the coherence time is comparable to the free evolution time, the gain obtained by using  $N=2$  NOON state is partially offset by the corresponding faster decoherence, and thus we failed to achieve phase super-sensitivity. It is expected that, our NOON state will show the desired phase super-sensitivity with the improvement of the coherence time.

In summary, we have proposed and demonstrated an entanglement assisted SW atom interferometer. In the experiment, phase super-resolution is clearly observed by exploiting the second order NOON state. Higher order SW NOON state with small  $N$  can be generated in current setup to further demonstrate the principle of quantum-enhanced-measurement. Besides, since the quantum memory is automatically built in our system,  $N$ -quanta SW GHZ state can be deterministically generated in a scalable way, which is a distinct advantage compared with photonic entanglement. The SW interferometer might be used as an inertial sensor by significantly improving several quantities, such as coherence time and retrieve efficiency of the quantum memory, and the detection efficiency. The coherence time of the quantum memory can be substantially extended by, e.g., further reducing the temperature or trapping the atoms in optical lattice [20]. The retrieval efficiency and the detection efficiency can be respectively improved by exploiting an optical cavity [21] and the photon-number-resolving detectors [22, 23].

We acknowledge J. Schmiedmayer for useful discussions. This work was supported by the Alexander von Humboldt Foundation, the European Commission through the ERC Grant and the STREP project HIP, the National Fundamental Research Program (Grant No.2006CB921900), the CAS, and the NNSFC.

- 
- [1] J. P. Dowling, Contemporary Physics **49**, 125 (2008).
  - [2] A. D. Cronin, J. Schmiedmayer and D. E. Pritchard, <http://arxiv.org/abs/0712.3703v1>.
  - [3] V. Giovannetti, S. Lloyd and L. Maccone, Science **306**, 1330 (2004).
  - [4] P. Walther *et al.*, Nature **429**, 158 (2004).
  - [5] M. Mitchell, J. Lundeen and A. Steinberg, Nature **429**, 161 (2004).
  - [6] T. Nagata *et al.*, Science **316**, 726 (2007).

- [7] H. Häffner *et al.*, Nature **438**, 643 (2005).
- [8] L.-M. Duan, M. D. Lukin, J. I. Cirac and P. Zoller, Nature **414**, 413 (2001).
- [9] P. Kok, H. Lee and J. P. Dowling, Phys. Rev. A **65**, 052104 (2002).
- [10] D. Greenberger, M. Horne and A. Zeilinger, *Bell's Theorem, Quantum Theory, and Conceptions of the Universe*, 69. Kluwer, Dordrecht (1989).
- [11] S. D. Barrett, P. P. Rohde and T. M. Stace, [Http://arxiv.org/abs/0804.0962v1](http://arxiv.org/abs/0804.0962v1).
- [12] D. E. Browne and T. Rudolph, Phys. Rev. Lett. **95**, 010501 (2005).
- [13] B. Zhao *et al.*, Nature Physics **5**, 95 (2009).
- [14] W. Wohlleben, F. Chevy, K. Madison and J. Dalibard, Eur. Phys. J. D **15**, 237 (2001).
- [15] Y.-A. Chen *et al.*, Nature Physics **4**, 103 (2008).
- [16] S. Chen *et al.*, Phys. Rev. Lett. **97**, 173004 (2006).
- [17] S. F. Huelga *et al.*, Phys. Rev. Lett. **79**, 3865 (1997).
- [18] M. Auzinsh *et al.*, Phys. Rev. Lett. **93**, 173002 (2004).
- [19] D. Leibfried *et al.*, Science **304**, 1476 (2004).
- [20] M. Greiner *et al.*, Nature **415**, 39 (2002).
- [21] J. Simon, H. Tanji, J. K. Thompson and V. Vuletić, Phys. Rev. Lett. **98**, 183601 (2007).
- [22] D. F. V. James and P. G. Kwiat, Phys. Rev. Lett. **89**, 183601 (2002).
- [23] A. Imamoglu, Phys. Rev. Lett. **89**, 163602 (2002).

## APPENDIX

**Measurement-induced NOON state.** Our measurement-induced NOON state in spin-wave (SW) interferometer method closely follows the scheme proposed by Nielsen and Mølmer [?], where the NOON state can be conditionally generated from two pulsed type II optical parametric oscillators with only linear optical devices. As shown in Supplementary Figure A1, two atom-light fields (mode  $a$  and  $b$ ) can be written as  $|\Psi\rangle_a \otimes |\Psi\rangle_b$ , where

$$|\Psi\rangle_i \sim \sum_N \sqrt{\chi_i^N} |N\rangle_i^s |N\rangle_i,$$

where  $\chi_i \ll 1$  is the excitation probability of one collective spin in SW  $i$  ( $i = a, b$ ),  $|N\rangle_i^s$  denotes the Stokes field  $S_i$  with photon number  $N$  and  $|N\rangle_i$  denotes the  $N$ -fold collective spin excitation in SW  $i$ . The two light fields from spontaneous Raman process selecting perpendicular polarization are guided on a polarized beam-splitter (PBS). By adjusting the two modes  $a$  and  $b$  to be equally excited ( $\chi_a = \chi_b = \chi$ ), the atom-light fields can be expressed as

$$|\Psi\rangle_a \otimes |\Psi\rangle_b \sim \left( \sum_N \sqrt{\chi^N} |V\rangle^{\otimes N} |N\rangle_a \right) + \left( \sum_N \sqrt{\chi^N} |H\rangle^{\otimes N} |N\rangle_b \right) \quad (\text{A.1})$$

From the Eq. A.1, by a projection measurement of the combined light field onto

$$|H\rangle^{\otimes N} - |V\rangle^{\otimes N}, \quad (\text{A.2})$$

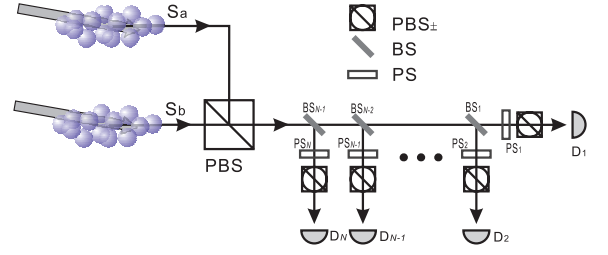


FIG. A1: Measurement-induced NOON state preparation in SW interferometer.  $BS_i$  denotes the beam-splitter with reflectivity of  $\frac{1}{i+1}$ . The phase shifters  $PS_j$  transform  $|V\rangle$  to  $-e^{i 2j\pi/N} |V\rangle$ .  $PBS_{\pm}$  are polarizing beam-splitters oriented at  $45^\circ$ , which reflects photons with  $|-\rangle$  polarization and transmits photons with  $|+\rangle$ . The coincidence between detectors  $D_1, D_2, \dots, D_N$  will project the SW interferometer onto the NOON state  $|NOON\rangle$  (Eq. A.3).

with  $H, V$  representing the horizontal and vertical polarization, the atom field (the SW interferometer) is projected onto the NOON state [A.2],

$$|NOON\rangle \sim |N\rangle_a |0\rangle_b - |0\rangle_a |N\rangle_b. \quad (\text{A.3})$$

To do so, we rewrite Eq. A.2 as,

$$|H\rangle^{\otimes N} - |V\rangle^{\otimes N} = \bigotimes_{n=1}^N (|H\rangle - |V\rangle e^{i 2n\pi/N}). \quad (\text{A.4})$$

From Eq. A.4, by properly setting the measurement device as shown in Supplementary Figure A1, the coincidence between detectors  $D_1, D_2, \dots, D_N$  will project the SW interferometer onto the NOON state  $|NOON\rangle$  (Eq. A.3). Note that, although our method for preparing NOON state is in principle extendable [A.3] to arbitrary  $N$ , the efficiency of generating the desired NOON state drops off exponentially [A.4] as a function of  $N$ .

In the experiment, to generate the second order NOON state in SW interferometer  $|2\rangle_a |0\rangle_b - |0\rangle_a |2\rangle_b$ , we need to perform the projection measurement of the Stokes field onto  $|H\rangle \otimes |H\rangle - |V\rangle \otimes |V\rangle = (|H\rangle + |V\rangle) \otimes (|H\rangle - |V\rangle)$ . This can be simply achieved by setting the HWP<sub>s</sub> in Fig. 1 at  $22.5^\circ$  and measuring the coincidence between detectors  $D_{S1}$  and  $D_{S2}$ . This would be the same as the complex measurement devices in Fig. A1 when  $N = 2$ . Note that, in our experiment, the excitation probability  $\chi \ll 1$ , and thus the contribution from higher order excitations can be safely neglected.

**Experimental cycles.** As shown in Fig. 1, in the experiment, the MOT is loaded for 20 ms at a repetition rate of 40 Hz. The trapping magnetic field and repumping beams are then quickly switched off. After 0.5 ms, the bias magnetic field of about 3 G is switched on, whereas the cooler beams is switched off and two pumping beams are switched on for 0.5 ms to optically pump the atoms to the desired state  $|g\rangle$ . As the two pumping beams, one couples all the magnetic transitions of  $|5S_{1/2}, F =$



$2\rangle \rightarrow |5P_{3/2}, F' = 2\rangle$  (not shown in the figure), shining with cooler light; the other pump ( $\pi$ -pump) couples the  $\pi$  transition  $|5S_{1/2}, F = 1\rangle \rightarrow |5P_{1/2}, F' = 1\rangle$ , shining in from the side. Then, within another 4 ms, experimental trials (each consisting of pumping, write and read pulses) are repeated with a controllable period depending on the desired retrieval time. In order to re-prepare the atoms to the desired state  $|g\rangle$ , we switch on the two pumping beams in each experimental trial before write and read process,  $|5S_{1/2}, F = 2\rangle \rightarrow |5P_{3/2}, F' = 2\rangle$  pump for 1.2  $\mu$ s and  $\pi$ -pump for 0.9  $\mu$ s.

To deterministically generate the second order NOON state, in each experimental run, we keep shining the write pulses. Following each write, the two pumping beams (clean pulses) are switched on to re-prepare the atoms to the initial state  $|g\rangle$ . A click of coincidence between detectors  $D_{S1}$  and  $D_{S2}$  in Fig. 1 will stop the remaining write pulses and clean pulses and the NOON state is induced in the SW interferometer. After the SW state is converted back to anti-Stokes photons, another experimental run restarts.

**Fitting the experimental results.** For the first order NOON state, considering the retrieval efficiency and the background noise, the probability of detecting one photon in detectors  $D_{AS1}$  and  $D_{AS2}$ , conditional on detecting a Stokes field on state  $|+\rangle$  are described by

$$\begin{aligned} p_{AS1} &= \gamma(\delta t) \cos^2(\Delta\phi(\delta t) + \phi_0) + \gamma_b, \\ p_{AS2} &= \gamma(\delta t) \sin^2(\Delta\phi(\delta t) + \phi_0) + \gamma_b, \end{aligned}$$

where  $\gamma(\delta t) = \gamma_0 \exp(-\delta t^2/\tau^2)$  is the overall retrieve efficiency,  $\phi_0 = -\frac{\phi_1 + \phi_2}{2}$  and  $\gamma_b$  denotes the background. The lifetime  $\tau$  for single SW excitation is measured from the decay from the correlation function as in Ref. [A.5]. The fidelity of anti-Stokes field on  $|+\rangle$  are calculated to be  $f_{+|+}(\delta t) = (0.5 + a \cos^2(\pi \frac{\delta t}{T} + \phi_0) e^{-\delta t^2/\tau^2}) / (1 + a e^{-\delta t^2/\tau^2})$ , with  $a = \frac{\gamma_0}{2\gamma_b}$  and  $T = \frac{\pi}{\Delta \mathbf{k} \cdot \mathbf{v}_c}$  the evolution period. Similarly, the fidelity of anti-Stokes field on  $|+\rangle$  on condition of a Stoke photon on state  $|-\rangle$  can be written as  $f_{+|-}(\delta t) = (0.5 + a \sin^2(\pi \frac{\delta t}{T} + \phi_0) e^{-\delta t^2/\tau^2}) / (1 + a e^{-\delta t^2/\tau^2})$ . The curves in Fig. 2 are joint fitting with

$f_{+|+}$  and  $f_{+|-}$ , where  $a$ ,  $T$  and  $\phi_0$  are fitting parameters.

For the second order NOON state, the coincidence count between  $D_{AS1}$  and  $D_{AS2}$  are measured, which can be described as

$$p_{AS1} = \frac{1}{2} \gamma^2(\delta t) \sin^2(2\Delta\phi(\delta t) + \phi'_0) + 2\gamma_b \gamma(\delta t) + \gamma_b^2,$$

where the first term is the two photon coincidence from the second order excitation, the second term is noise coming from the coincidence between the excitation and the background, and the third term is the coincidence between background noise. The normalized data are the coincidence counts divided by the sweeps, and are fitted by using

$$c(\delta t) = b \sin^2\left(\pi \frac{\delta t}{T'} + \phi'_0\right) e^{-2\delta t^2/\tau^2} + d e^{-\delta t^2/\tau^2},$$

where we neglect the coincidence from background noise for simplicity,  $\tau$  is the lifetime of the spin wave obtained from the decay from correlation,  $b$ ,  $d$ ,  $\phi'_0$  and  $T' = \frac{\pi}{2\Delta \mathbf{k} \cdot \mathbf{v}_c}$  are fitting parameters. Note that, from the first order data, we know that the background noise is much smaller than the signal retrieved from the atom ensemble. Thereby for the second order NOON state, the background coincidence count can be safely neglected since it is the second order small term. This does not affect the conclusion of our paper, since the lack of super-sensitivity in our experiment is mainly caused by short coherence time of the SW.

- 
- [A.1] A. E. B. Nielsen, K. Mølmer, *Phys. Rev. A* **75**, 063803 (2007).
  - [A.2] F. W. Sun, Z. Y. Ou, G. C. Guo, *Phys. Rev. A* **73**, 023808 (2006).
  - [A.3] P. Walther, *et al.*, *Nature* **429**, 158 (2004).
  - [A.4] P. Kok, H. Lee, J. P. Dowling, *Phys. Rev. A* **65**, 052104 (2002).
  - [A.5] B. Zhao, *et al.*, *Nature Physics* **5**, 95 (2009).